DMD Fast Forward. Published on April 12, 2012 as doi:10.1124/dmd.112.044925

DMD #44925

Nano-advantage in Enhanced Drug Delivery with Biodegradable Nanoparticles: Contribution of Reduced Clearance

Rajendra S. Kadam, David W. A. Bourne, and Uday B. Kompella

Nanomedicine and Drug Delivery Laboratory, Department of Pharmaceutical Sciences (R.S.K., D.W.A.B., and UBK)

Department of Ophthalmology, and Bioengineering (U.B.K.)

University of Colorado Anschutz Medical Campus, Aurora, CO 80045

Department of Pharmaceutical Sciences, University of Oklahoma, Oklahoma City, OK (D.W.A.B.)

DMD Fast Forward. Published on April 12, 2012 as DOI: 10.1124/dmd.112.044925
This article has not been copyedited and formatted. The final version may differ from this version.

Running Title: Pharmacokinetics of Biodegradable Nanoparticles

Corresponding author: Uday B Kompella, Ph.D., Department of Pharmaceutical Sciences, University of Colorado Anschutz Medical Campus, 12850 E. Montview Blvd, Aurora, CO 80045 (Phone: 303-724-4028 ; Fax: 303-724-4666 ; E-mail: uday.kompella@ucdenver.edu)

Number of text pages: 32
Number of tables: 1
Number of figures: 7
Number of references: 53
Number of words in abstract: 166
Number of words in introduction: 823
Number of words in discussion: 2073

List of abbreviations:

GIT: gastrointestinal tract; AIC: Akaike information criteria; PK : Pharmacokinetics ; AUC : Area under plasma concentration time curve; kel: Elimination rate constant from the plasma compartment; k12: Rate constant for transfer of drug from the plasma compartment to the distribution compartment; k21: Rate constant for transfer of drug from the distribution compartment to the plasma compartment; CL: clearance ; V: volume of distribution.

Abstract

The aim of this study was to investigate the contribution of reduced apparent clearance to the enhanced exposure reported for biodegradable nanoparticles after extravascular and intravascular routes of administration. Plasma concentration profiles for drug and nanoparticle formulations following administration by intravenous, intraduodenal, and oral routes were extracted from literature. Data were fit to pharmacokinetic models using Boomer. The compartmental pharmacokinetic analysis of literature data for six drugs including camptothecin, 9-nitrocamptothecin, epirubicin, vinpocetine, clozepine, and cyclosporine-A showed that the encapsulation of drug molecules in nanoparticles significantly reduced the apparent clearance and prolonged the apparent circulation half-life compared with the plain drug. Positively charged nanoparticles assessed in this study had lower apparent clearance, lower elimination rate constant values and longer apparent circulation half-life than neutral and negatively charged nanoparticles. Following oral administration, a reduction in apparent clearance contributed substantially to elevations in plasma drug exposure with nanoparticles. For the drugs and delivery systems examined, the nano-advantage in drug delivery enhancement can be explained, in part, by reduced clearance.

DMD Fast Forward. Published on April 12, 2012 as DOI: 10.1124/dmd.112.044925
This article has not been copyedited and formatted. The final version may differ from this version.

Introduction

Drug encapsulating nanoparticles or nanosystems in general have been reported to enhance delivery to target tissue due to increased drug permeability or absorption (Gelperina et al., 2005; Mishra et al., 2008), thereby reducing the dosing frequency and improving patient compliance (Gelperina et al., 2005; Emerich and Thanos, 2006; Bawa, 2008; Zhang et al., 2009). Nanoparticles also minimize the side effects (Sinha et al., 2006; Zhang et al., 2008) and sustain the drug release over prolonged period of time. Nano-delivery systems are being developed for various drug molecules. Although several of the above advantages are feasible in general, enhanced permeability based absorption with nanoparticles is debatable as the sole or primary contributor to the nanoparticles delivery advantage observed in several of the previous studies. Typically, studies based on nanosystems assess a single time point or an incomplete concentration versus time profile and conclude enhanced drug absorption or delivery. In such studies, dissecting the contribution of enhanced absorption versus reduced clearance is not possible. Even in studies where the entire concentration-time course is obtained, the assumption of enhanced absorption is made without fully considering the contribution of reduced clearance (El-Shabouri, 2002; Italia et al., 2007). Typically, drug exposure is measured as area under the concentration versus time curve (AUC) in target tissues or a surrogate tissue such as plasma. AUC can be increased due to an increase in fraction absorbed or due to a decrease in clearance rate. Reduction in clearance typically contributes to elevated AUC but may be incorrectly attributed to enhanced absorption. Therefore, the purpose of this study was to determine the contribution of reduced clearance to enhanced delivery or drug exposure measured as AUC in several previously reported studies (El-

Shabouri, 2002; Manjunath and Venkateswarlu, 2005; Luo et al., 2006; Schluep et al., 2006; Dadashzadeh et al., 2008; Li et al., 2010).

Nano-formualtion may enhance absorption by increasing the gastric residence time through mucosal adhesion (Takeuchi et al., 1996) or by increasing cell or tissue entry (e.g., Peyer's patches and M cell mediated uptake) (Florence AT et al., 1995a; Florence AT et al., 1995b; Torche´ AM et al., 2000; Florence AT, 2005). An additional barrier for drug absorption is chemical and metabolic instability of the drug. GIT is rich in phase-I and phase-II metabolic enzymes. Drugs such as cyclosporine-A (Italia et al., 2007), estradiol (Mittal et al., 2007), and curcumin (Anand et al., 2007) exhibit chemical or enzymatic instability in the GIT. Many drug molecules have lower systemic bioavailability after oral administration, because of enzymatic and nonenzyamtic degradation in the gastrointestinal tract (GIT) and first-pass metabolism in the liver before the drug reaches the systemic circulation (Italia et al., 2007; Mittal et al., 2007). Nanoparticle formulations can reduce the drug exposure to the adverse conditions in the GIT, thereby minimizing the enzymatic and non-enzymatic degradations; this can lead to an increase in AUC or drug exposure.

Intravenously administered hydrophilic drug molecules typically undergo rapid renal clearance because of poor reabsorption after glomerular filtration(Lin and Lu, 1997); whereas, lipophilic drugs tend to undergo biotransformation in the liver to hydrophilic metabolites prior to biliary or renal excretion(Parkinson A. et al., 2010). Encapsulation of drug in nanoparticles reduces renal clearance because of increased size (cutoff for renal clearance is < 15 nm) (Choi H, 2007). Further, nanoparticle formulations

may protect lipophilic drugs from metabolizing enzymes in the liver (Li and Huang, 2008).

Most of the reported studies observed an increase in the area under the plasma concentration versus time curve (AUC) or drug exposure for drug encapsulated in nanoparticles when compared to the plain drug solution or suspension administered by the same route. After intravenous administration, it is possible to identify the contribution of reduced total drug clearance to enhanced drug exposure by nanoparticle formulation. For extravascular routes of administration, assessing contribution of reduced clearance versus enhanced absorption becomes more difficult. Previous literature reports made strong statements that an increase in delivery with nanoparticles when compared to plain drug solution or suspension was due to enhanced uptake from the site of administration (Hussain et al., 1997; El-Shabouri, 2002; Qian et al., 2006; Italia et al., 2007). Although these conclusions may be true in part, these studies did not consider the effect of reduced clearance from plasma or at the site of administration as a contributor to enhanced drug exposure. There are no reports that systematically determined the contribution of reduced clearance to nanoparticles mediated enhancement in drug exposure. Part of the difficulty, as elaborated through this study, includes lack of available methods to analyze free drug, nanoparticle bound drug, and protein bound drug in the tissues of interest.

The objective of the present study was to develop pharmacokinetic (PK) models for plain drug and nanoparticle encapsulated drug after oral, intra-duodenal, and intravenous routes of administration and to understand the influence of altered drug clearance on enhanced drug exposure with nanoparticle formulations. Further, efforts

were made to understand the influence of nanoparticle surface charge on plasma pharmacokinetics.

Method

Dataset for modeling

The datasets used in this study were collected from the literature for six drug molecules. Data pertaining to the plasma concentration profile after single dose administration of plain drug formulation and nanoparticle formulation from the same study were only considered for analysis. The plasma concentration data was extracted from the plasma concentration profile graphs provided in the literature so standard deviations were not available. Due to the limitation of currently available bioanalytical methods, published reports used for this study did not distinguish free drug, nanoparticle bound drug, and protein bound drug. These earlier studies reported total drug concentration, which was used in the present study. The parameter estimates obtained for nanoparticles is combination of both released plain drug as well as drug in nanoparticles. Therefore, the parameters estimated for the nanosystems should be considered as apparent clearance, apparent volume of distribution and apparent circulation half-life. Nanoparticle literature commonly uses the term circulation half-life as a synonym for terminal half-life (Petros and DeSimone, 2010). Hence, we use the term circulation half-life in this report.

Modeling software

The mathematical compartmental modeling was performed using the Boomer, a differential and integrated equation based modeling program (Bourne, 1989). The parameters for each compartmental model were estimated using the simplex damping Gauss-Newton curve-fitting procedure in this software. Numerical integration was performed using the Runge-Kutta-Fehlberg 45 method for all analyses.

Model development

PK model development was started as a forward stepwise approach as in the multiple linear regression. Initial model was developed as the simplest model based on the route of administration. For the oral route of administration, both absorption and elimination processes were considered as first order process. A distribution compartment was added to the initial model when necessary to improve the fit to the data. Data were weighted using two weighting scheme, equal weight and by $1/Cp(i)^2$. The final best fit model was selected based on Akaike information criteria (AIC), parameter coefficients of variation (% CV), visual inspection of the weighted residual plots and concentration versus time plots, and coefficient of regression (R^2). Lower AIC values, lower coefficient of variation (% CV), weighted residual plot with random distribution, and higher coefficient of regression (R^2) indicated a better fit to the data and model selection. Between the two weighting schemes used, $1/Cp(i)^2$ showed better random distribution of data in weighted residual plots for all drugs compared with the equal weight scheme; hence, $1/Cp(i)^2$ weighting scheme was used for all selected models.

Results

Data collection

Literature reports on the plasma concentration profiles for plain drug and nanoparticle formulations were chosen for six drug molecules administered by three different routes of administration, i.e., oral, intraduodenal and intravenous. Table 1 summarizes the drug name, particle size, surface charges, route of administration, species of study, and dose of drug. Except camptothecin IT-101, which is a soluble conjugate, all other nano-formulations are particle dispersions. To compare the effect of nano-formulation on pharmacokinetic parameters, compartmental modeling was carried out after intravenous, intraduodenal, and oral administrations and compared with plain drug formulation. To study the effect of surface charge of nanoparticles on pharmacokinetic parameters, the pharmacokinetic profiles of positive, negative, and neutral nanoparticles were assessed. The dataset contained only the small drug molecules and not the macromolecules such as proteins and plasmids because of the paucity of PK profile data for macromolecules encapsulated in nanoparticles.

Pharmacokinetic modeling after intravenous administration

Intravenous data were available for camptothecin solution and its polymer conjugate, 9-nitrocamptothecin solution and nanoparticles, and epirubicin solution and nanoparticles. For camptothecin, a single compartment model showed a poor fit to the data for both drug solution and the polymer conjugate (AIC = 6.6, -6.6 respectively). Addition of a second distribution compartment improved the fit significantly for drug solution and nanoparticles (AIC = -14.3, -9.3 respectively). The best-fit model along with a PK parameter summary is given in Figure 1. Polymer-drug conjugate showed 266 fold

lower apparent plasma clearance, 11 fold lower apparent volume of distribution and 19 times longer apparent circulation half-life than plain drug.

For 9-nitrocamptothecin, a single compartment model provided a good fit for drug solution (AIC = -20.2) and a reasonable fit for nanoparticles (AIC = 1.16). Addition of a distribution compartment resulted in a significant improvement in the fit to the data for nanoparticles with a significant reduction of AIC values (AIC = -10.4). Comparison of PK parameters showed that nanoparticles had a 5.4 fold lower apparent clearance, 7.1 fold lower apparent volume of distribution and 2.6 times longer apparent circulation half-life (Figure 2).

For epirubicin solution and nanoparticles, single compartment model showed a poor fit to the data (AIC = 1.2, 6.6 respectively); however, addition of a distribution compartment data improved the fit significantly for the solution (AIC = -7.7). For epirubicin nanoparticles, addition of second compartment improved the fit (AIC = -12.6), but visual observation of the weighted residual plot and concentration time plot suggested a model with three compartments might be better model. Addition of second distribution compartment resulted in a significant improvement in the fit (AIC = -23.3) for epirubicin nanoparticles when compared to the one and two compartment models (Figure 3). Comparison of PK parameters for the final selected models showed that the nanoparticles had 11.9 fold lower apparent clearance, 1.2 fold lower apparent volume of distribution, and 7.2 times longer apparent circulation half-life (Figure 3).

Pharmacokinetic modeling after oral administration

Datasets for two drug molecules administered either orally or intra-duodenally as solution or suspension and their nanoparticles were used for PK modeling. The model

development was started with one compartment extravascular administration, with drug dosing in GI compartment. A distribution compartment was added when necessary to achieve the best-fit.

For vinpocetine drug solution and nanoparticles, the pharmacokinetic compartmental modeling was started with a one-compartment model describing GIT and blood compartment and elimination from the blood compartment. For vinpocetine solution, a one compartment model showed a better fit than a two compartment model (AIC= -10.8, -6.8 respectively), but the predicted maximum concentration (Cmax) was lower than the observed one. Addition of a lag time component to the one compartment model for vinpocetine solution improved the fit significantly (AIC = -15.4) and the predicted Cmax value was closer to observed value (Figure 4). For vinpocetine nanoparticles, a two compartment model with lag-time (Figure 4) provided a better fit to the data than a one compartment model (AIC = -23.1 versus-16.4). Comparisons of the PK parameters for the final selected models showed that incorporation of drug in nanoparticles results in 4.5 fold lower apparent clearance (CL/F), 1.7 fold lower apparent volume of distribution (V/F), and 1.8 times longer apparent circulation half-life (Figure 4) than the plain drug .

For clozepine drug suspension and nanoparticles, the data was available for both intravenous and intraduodenal administration. The compartmental modeling was performed using simultaneous fit to the intraduodenal and intravenous plasma data. All the PK parameters except absorption rate constant (ka) and fraction absorbed (F) were common for both intraduodenal and intravenous data. After intravenous administration, both nanoparticles and suspension could be explained well by a two compartmental

model, and therefore, simultaneous fit was performed using a two compartmental model. Model predicted and observed data fit along with comparisons of PK parameters for the final selected models are given in Figure 5. As shown in Figure 5, incorporation of drug in nanoparticles results in 2.95 fold lower apparent clearance (CL), 1.74 fold lower apparent volume of distribution (V), 1.7 times longer apparent circulation half-life, 2.1 fold higher apparent absorption rate constant (ka), and 1.5 fold higher fraction absorbed (F).

Effect of surface charge of nanoparticles on absorption and elimination

To investigate the effect of surface charge of nanoparticles on PK profile, compartmental modeling was carried out on positively and negatively charged cyclosporine-A (CsA) nanoparticles administered orally and positively and neutrally charged nanoparticles of clozepine administered intraduodenally and intravenously. The two compartment models showed a better fit to the data after the oral route of administration for both clozepine nanoparticles and cyclosporine-A nanoparticles (Figures 6 and 7). Comparison of PK parameters for the final selected model for clozepine nanoparticles are given in Figure 6. After intravenous administration, neutral clozepine nanoparticles showed 2-fold higher apparent clearance and 2-fold lower apparent circulation half-life compared to positively charged nanoparticles (Figure 6). After intraduodenal administration, negatively charged nanoparticles had 2.3-fold higher apparent clearance (CL/F) and 5.3-fold lower apparent circulation half-life than positively charged clozepine nanoparticles. Comparisons of PK parameters for the final selected models for cyclosporine-A nanoparticles are given in Figure 7. For cyclosporine-A, negatively charged nanoparticles exhibited 3-fold higher apparent plasma oral

DMD Fast Forward. Published on April 12, 2012 as DOI: 10.1124/dmd.112.044925
This article has not been copyedited and formatted. The final version may differ from this version.

clearance (CL/F) and 3 fold lower apparent circulation half-life ($t_{1/2}$) when compared with the positively charged nanoparticles. Differences in the apparent absorption rate constant (ka) were not as large (1.45 fold higher for positively charged nanoparticles).

Discussion

The relative role of enhanced uptake/absorption versus reduced clearance on enhanced delivery and efficacy achieved by biodegradable, drug loaded nanoparticles is unclear. It is generally assumed that the enhanced uptake/absorption is responsible for the enhanced delivery and efficacy observed with nanoparticles. In this study, based on compartmental pharmacokinetic analysis of literature data for drug disposition following administration of plain drug and nanoparticle formulations by oral, intra-duodenal, and intravenous routes of administration, we assessed the contribution of changes in absorption and clearance to the delivery of 6 drug molecules. We observed that the total body apparent clearance and the elimination rate constants were several-fold lower for the drug encapsulated in nanoparticle formulations than the plain drug after oral, intra-duodenal, and intravenous administrations. Effect of nanoparticle formulation on the absorption rate constant after oral administration was less substantial. Further, our analysis also shows that positively charged nanoparticles evaluated in this study offer lower apparent clearance and elimination rate constant, and hence longer apparent circulation half-life and higher plasma AUC. These findings are further elaborated below.

Some of the previous literature reports showed rapid clearance and very short circulation half-life for nano- and micro- systems after intravenous administration when compared to plain drug (Grislain L et al., 1983; Verrecchia T. et al., 1995). Keeping the rapid clearance of nanoparticles in mind, many investigators may have interpreted enhanced efficacy of nanosystems as a result of enhanced uptake in the target organ. Various attempts were made in the literature to prolong the circulation half-life for nanoparticles. Some examples include the use of polyethylene glycol (PEG), polyvinyl

alcohol (PVA), polysaccharides, and surfactants such as poloxmer to coat the surface of nanosystems to reduce the opsonization and clearance by the reticuloendothelial system (Papahadjopoulos et al., 1991; Gref et al., 1994; Slepushkin et al., 1997). Based on these developments and pharmacokinetic principles, it is critical to dissect the contributions of reduced drug clearance (measured as changes in total body clearance and/or apparent elimination rate constant) and enhanced absorption (measured as apparent rate constant for absorption or fraction absorbed) to enhanced drug delivery achieved by nanosystems.

To determine the contribution of change in apparent clearance to plasma pharmacokinetics, compartmental modeling was carried out on plain drug as well as nanosystems of camptothecin, 9-nitrocamptothecin, and epirubicin after intravenous administration (Figures 1, 2, and 3). Entrapment of these drugs in nanosystems resulted in reduced apparent clearance, longer apparent circulation half-life, and lower apparent volume of distribution, leading to protracted drug exposure or AUC in the plasma. Since apparent volume of distribution is lower for nanoparticles when compared to the drug, longer apparent circulation half-life does not appear to be a result of rapid deposition of nanoparticles in tissues followed by slow drug redistribution to blood. Further, distribution compartment parameters k12 and k21 were lower for nanoparticles than plain drug after intravenous administrations indicating slower distribution of drug to peripheral tissues for nanoparticles when compared to the plain drug (Figures 1 and 3). Due to large size of nanoparticles, small gaps between endothelial cells of blood vessels in peripheral tissues hinder the delivery of nanoparticles, resulting in reduced apparent volume of distribution for nanoparticles than plain drugs. For camptothecin and 9-

nitorcamptothecin, nanosystems exhibited 11- and 7- fold lower apparent volumes of distribution compared to the plain drugs (Figures 1 and 2).

Clinical applicability of camptothecin was limited by instability of the lactone ring, which rapidly hydrolyzes in vivo to inactive carboxylate metabolite (Scott et al., 1993; Schluep et al., 2006). Conjugation of camptothecin to cyclodextrin based polymer (IT-101) reduces metabolic clearance by increasing chemical stability of the lactone ring and reduces renal clearance by increasing the size, thereby prolonging the circulation half-life (Schluep et al., 2006). Similar to camptothecin, 9-nitrocamptothecin has the lactone ring instability (Chow et al., 2000). Further, 9-nitrocamptothecin undergoes phase-I and phase-II hepatic metabolism (Li et al., 2003). Encapsulation of drug in polymeric nanoparticles imparted both chemical as well as metabolic stability to 9-nitrocamptothecin, resulting in reduced hepatic clearance and prolonged circulation half-life (Dadashzadeh et al., 2008). Epirubicin, an antineoplastic drug undergoes extensive hepatic metabolism (Gurney et al., 1998), and encapsulation of drug in nanoparticles reduces its hepatic clearance.

Nanoparticles are widely gaining attention as drug delivery systems for oral administration of drugs having poor oral bioavailability. In addition to enhancing drug absorption through cell mediated uptake (Florence AT, 2005), drug loaded nanoparticles can reduce the transporter mediated efflux (Ling et al., 2010). Further drug entrapment in nanoparticles protects the drug from degradation by adverse conditions in gastrointestinal tract (Italia et al., 2007; Mittal and Kumar, 2009) and reduces hepatic first-pass metabolism (Anand et al., 2007; Mittal et al., 2007). Protection of drug from degradation/metabolism in the gastrointestinal tract and liver reduces the metabolic

clearance and enhances the apparent rate constant for absorption and fraction absorbed. At times in literature, the enhanced delivery with nanoparticles after oral administration was translated as a consequence of enhanced permeability processes (El-Shabouri, 2002; Gelperina et al., 2005; Luo et al., 2006; Mittal et al., 2007). We performed plasma pharmacokinetic analysis for orally administered nanoparticles and plain drug formulations of vinpocetine and clozepine in order to determine the contribution of reduced clearance to enhanced drug delivery observed with nanoparticles (Figure 4 and 5). With oral or duodenal administration, the nanoparticles showed lower apparent clearance, lower apparent volume of distribution, lower elimination rate constant, longer apparent circulation half-life, and higher plasma AUC than the plain drug administered as solutions or suspensions of vinpocetine and clozepine respectively (Figures 4 and 5). For vinpocetine nanoparticles, the plasma concentration profile was available only for the oral route of administration; hence dissection of clearance and volume of distribution from fraction observed (F) was not possible. Nanoparticle encapsulation of vinpocetine results in a 4.5-fold reduction in apparent clearance (CL/F), 1.7–fold lower apparent volume of distribution (V/F), while there was 2.6-fold increase in apparent absorption rate constant (ka). After oral administration, vinpocetine undergoes extensive first pass metabolism, resulting in low bioavailability (< 7%) (El-Laithy et al., 2011). Further, absorbed drug undergoes extensive hepatic metabolism and unchanged vinpocetine could not be detected in urine (Vereczkey et al., 1979). Incorporation of vinpocetine in solid-lipid nanoparticles protected it from enzymatic degradation and reduced its metabolic clearance (Luo et al., 2006). In case of clozepine, plasma concentration profiles were available after both intravenous and intraduodenal administration of nanoparticles and

plain drug suspension. Simultaneous model fitting of intraduodenal and intravenous plasma concentration profile gives fraction absorbed (F), apparent clearance (CL), and apparent volume of distribution (V) (Figure 6). Clozepine nanoparticles showed 1.5- fold higher fraction absorbed (F), 3.0- fold lower apparent clearance (CL), and 1.7- fold lower apparent volume of distribution than plain drug suspension after intraduodenal administration (Figure 5). Clozepine is a lipophilic molecule that is rapidly absorbed after oral administration but undergoes extensive first-pass hepatic metabolism, resulting in poor oral bioavailability (< 30 %). Solid-lipid nanoparticles of clozepine can be absorbed through the lymphatic duct and bypass the presystemic hepatic metabolism to an extent following oral administration (Bargoni et al., 1998). However, clozepine in blood circulation undergoes extensive metabolic clearance, resulting in low plasma half-life (4.8 hr for plain clozepine versus 8.7 hr for nanoparticles). Results from clozepine nanoparticle pharmacokinetics clearly show that orally administered clozepine nanoparticles enhance drug exposure to the system, in part, by reducing metabolic clearance.

Nanoparticles surface properties including surface charge, hydrophobicity, and functional groups are key determinants of their biological fate. Levchenko and group showed that negatively charged liposomes (200 nm) have higher plasma clearance than the neutral liposomes (Levchenko et al., 2002). On the other hand, according to Kataoka (Yamamoto Y et al., 2001) and Roser (Roser et al., 1998) surface charge has no effect on plasma clearance of PEG-PLA micelles (37-39 nm) and albumin nanoparticles (500-600 nm), respectively. Piskin (Piskin et al., 1994) showed that positively charged polystyrene microparticles with primary amines have higher phagocytosis and nonspecific

internalization compared with the negatively charged microparticles. In this prior literature, it was hypothesized that positively charged nanoparticles have high nonspecific internalization and short blood circulation half-life (Alexis et al., 2008). Many attempts have been made to investigate the effect of surface charges of nanoparticle on pharmacokinetics and tissue distribution but the controversy remains. To study the effect of surface charge of nanoparticles on absorption versus clearance, PK modeling was carried for positively and negatively charged cyclosporine-A nanoparticles after oral administration in dogs and for positively and neutrally charged solid lipid nanoparticles of clozepine after intraduodenal and intravenous administrations in rats. Compartmental modeling of these two drugs with three different routes of administration unambiguously showed that positive surface charge result in reduced apparent clearance and longer apparent circulation half-life when compared to the neutral and negatively charged nanoparticles (Figure 6 and 7). After oral route of administration, positively charged nanoparticles clozepine and cyclosporine-A exhibited 3.0- to 5.3-fold longer apparent circulation half-life, respectively, than negative and neutral nanoparticles of these drugs (Figure 6 and 7). After intravenous administration, positively charged clozepine nanoparticles has 2.0- fold longer apparent circulation half-life and 1.9- fold lower apparent clearance than neutral charged nanoparticles. Recently Xu et al. (Xu et al., 2009) also showed that cationic nanoparticles have 9- and 31- fold longer circulation half-life than untreated and anionic polymeric nanoparticles after intravenous administration in rats. Another literature report also showed the accumulation of anionic liposomes in liver and spleen (Chonn et al., 1992).

Although we tried to dissect the contribution of various pharmacokinetic parameters to enhanced delivery with nanosystems, our study has its limitations. The plasma concentration profiles used in this study do not distinguish free drug, nanoparticle bound drug, and protein bound drug. Thus, the pharmacokinetic measures of this study are apparent values based on the total drug concentrations measured in the nanosystem groups. Further, the amount of drug bound to plasma proteins may be reduced by the nanoparticle formulation. Alternatively, particles may bind plasma proteins, altering particle size as well as changing the drug release profile in vivo. Drug encapsulated in nanoparticles is usually inactive, and requires drug release for activity at the target site (Li and Huang, 2008). Failure to release the active drug molecule at the target site is one possible reason for clinical failure of nanoparticle formulations. One example is the cisplatin liposomal formulation (SPI-077). Tumor cisplatin levels were four-fold higher for SPI-077 than plain cisplatin, but the formulation failed to exert its anticancer activity, because of failure to release cisplatin from the liposomes (Harrington et al., 2001; Andresen et al., 2005). Thus, precautions need to be taken when correlating enhanced delivery of nanoparticle formulation to efficacy.

Dissection of the contribution of released versus nanoparticle bound drug on pharmacokinetics using simulation is one approach to understanding the in vivo pharmacokinetics; however, development of simulation models for nanoparticle pharmacokinetics is limited by in vivo complexity. In addition to the drug being present in multiple forms including free drug, plasma protein or tissue bound drug, and nanoparticle bound drug, drug release from polymeric nanoparticles generally exhibits a triphasic release profile. The first phase is burst release governed by fast release of

surface adsorbed drug, the second phase is first order diffusion of drug from polymeric matrix, and the third phase is first order release due to degradation of polymeric matrix) (Zweers et al., 2006). Since the drug released from nanoparticle will very likely exhibit pharmacokinetic parameters similar to plain drug dosing, the pharmacokinetic parameters reported for nanoparticle groups in this study should be considered as apparent values. Further, in vivo clearance and distribution of nanoparticles is governed by various factors including nanoparticle material, size, shape, hydrophilicity, surface charge, and surface chemistry. Alexis et al., have reviewed the factors affecting on clearance and distribution of polymeric nanoparticles in vivo (Alexis et al., 2008).

In summary, we have shown the influence of reduced apparent clearance on enhanced exposure reported for various nanoparticles using pharmacokinetic modeling. We have suggested that encapsulation of drug molecules in nanoparticles significantly reduces the apparent drug clearance from plasma, thereby enhancing the apparent drug circulation half-life and potential cumulative drug delivery to the target tissues. Further we have suggested that some positively charged nanoparticles have longer apparent circulation half-life and reduced plasma clearance than neutral and negatively charged nanoparticles, resulting in better delivery. In addition to reduced clearance in the lumen of the gastrointestinal tract, liver, and circulation, it is anticipated that reduced clearance from tissues at the site of administration or absorption may also contribute to enhanced drug exposure with nanoparticles.

Authorship Contributions

Participated in research design: Kadam and Kompella.

Conducted experiments: Kadam, Bourne and Kompella.

Contributed new reagents: None

Performed data analysis: Kadam, Bourne and Kompella.

Wrote or contributed to the writing of the manuscript: Kadam, Bourne, and Kompella.

References

Alexis F, Pridgen E, Molnar LK and Farokhzad OC (2008) Factors affecting the clearance and biodistribution of polymeric nanoparticles. *Mol Pharm* **5:**505-515.

Anand P, Kunnumakkara AB, Newman RA and Aggarwal BB (2007) Bioavailability of curcumin: problems and promises. *Mol Pharm* **4:**807-818.

Andresen TL, Jensen SS and Jorgensen K (2005) Advanced strategies in liposomal cancer therapy: problems and prospects of active and tumor specific drug release. *Prog Lipid Res* **44:**68-97.

Bargoni A, Cavalli R, Caputo O, Fundaro A, Gasco MR and Zara GP (1998) Solid lipid nanoparticles in lymph and plasma after duodenal administration to rats. *Pharm Res* **15:**745-750.

Bawa R (2008) Nanoparticle-based therapeutics in humans: a survey. *Nanotechnology Law & Business* **5:**135-155.

Bourne DW (1989) BOOMER, a simulation and modeling program for pharmacokinetic and pharmacodynamic data analysis. *Comput Methods Programs Biomed* **29:**191-195.

Choi H LW, Misra P, Tanaka E, Zimmer J. P, Ipe B I, Bawendi M G, and Frangioni J V. (2007) Renal Clearance of Nanoparticles. *Nat Biotechnol* **25:**1165-1170.

Chonn A, Semple SC and Cullis PR (1992) Association of blood proteins with large unilamellar liposomes in vivo. Relation to circulation lifetimes. *J Biol Chem* **267:**18759-18765.

Chow DS, Gong L, Wolfe MD and Giovanella BC (2000) Modified lactone/carboxylate salt equilibria in vivo by liposomal delivery of 9-nitro-camptothecin. *Ann N Y Acad Sci* **922:**164-174.

Dadashzadeh S, Derakhshandeh K and Shirazi FH (2008) 9-nitrocamptothecin polymeric nanoparticles: cytotoxicity and pharmacokinetic studies of lactone and total forms of drug in rats. *Anticancer Drugs* **19:**805-811.

El-Laithy HM, Shoukry O and Mahran LG (2011) Novel sugar esters proniosomes for transdermal delivery of vinpocetine: preclinical and clinical studies. *Eur J Pharm Biopharm* **77:**43-55.

El-Shabouri MH (2002) Positively charged nanoparticles for improving the oral bioavailability of cyclosporin-A. *Int J Pharm* **249:**101-108.

Emerich DF and Thanos CG (2006) The pinpoint promise of nanoparticle-based drug delivery and molecular diagnosis. *Biomol Eng* **23:**171-184.

Florence AT (2005) Nanoparticle uptake by the oral route:fuilling its potential? *Drug Discovery Today: Technologies | Drug delivery/formulation and nanotechnology* **2:**75-81.

Florence AT, Hillery AM, Hussain N and Jani PU (1995a) Factors affecting the oral uptake and translocation of polystyrene nanoparticles: histological and analytical evidence. *Journal of Drug Targeting* **3:**65-70.

Florence AT, Hillery AM, Hussain N and Jani PU (1995b) Nanoparticles as carriers for oral peptide absorption:studies on particle uptake and fate. *Journal of Controlled Release* **36:**39-46.

Gelperina S, Kisich K, Iseman MD and Heifets L (2005) The potential advantages of nanoparticle drug delivery systems in chemotherapy of tuberculosis. *Am J Respir Crit Care Med* **172:**1487-1490.

Gref R, Minamitake Y, Peracchia MT, Trubetskoy V, Torchilin V and Langer R (1994) Biodegradable long-circulating polymeric nanospheres. *Science* **263:**1600-1603.

Grislain L, Couvreur P, Lenaerts V , Roland M, Deprez-Decampeneere D and Speiser P (1983) Pharmacokinetics and distribution of a biodegradable drug-carrier. *International Journal of Pharmaceutics* **15:**335-345.

Gurney HP, Ackland S, Gebski V and Farrell G (1998) Factors affecting epirubicin pharmacokinetics and toxicity: evidence against using body-surface area for dose calculation. *J Clin Oncol* **16:**2299-2304.

Harrington KJ, Lewanski CR, Northcote AD, Whittaker J, Wellbank H, Vile RG, Peters AM and Stewart JS (2001) Phase I-II study of pegylated liposomal cisplatin (SPI-077) in patients with inoperable head and neck cancer. *Ann Oncol* **12:**493-496.

Hussain N, Jani PU and Florence AT (1997) Enhanced oral uptake of tomato lectin-conjugated nanoparticles in the rat. *Pharm Res* **14:**613-618.

Italia JL, Bhatt DK, Bhardwaj V, Tikoo K and Kumar MN (2007) PLGA nanoparticles for oral delivery of cyclosporine: nephrotoxicity and pharmacokinetic studies in comparison to Sandimmune Neoral. *J Control Release* **119:**197-206.

Levchenko TS, Rammohan R, Lukyanov AN, Whiteman KR and Torchilin VP (2002) Liposome clearance in mice: the effect of a separate and combined presence of surface charge and polymer coating. *Int J Pharm* **240:**95-102.

Li K, Chen X, Zhong D and Li Y (2003) Identification of the metabolites of 9-nitro-20(S)-camptothecin in rats. *Drug Metab Dispos* **31:**792-797.

Li L, Gao FP, Tang HB, Bai YG, Li RF, Li XM, Liu LR, Wang YS and Zhang QQ (2010) Self-assembled nanoparticles of cholesterol-conjugated carboxymethyl curdlan as a novel carrier of epirubicin. *Nanotechnology* **21:**265601.

Li SD and Huang L (2008) Pharmacokinetics and biodistribution of nanoparticles. *Mol Pharm* **5:**496-504.

Lin JH and Lu AY (1997) Role of pharmacokinetics and metabolism in drug discovery and development. *Pharmacol Rev* **49:**403-449.

Ling G, Zhang P, Zhang W, Sun J, Meng X, Qin Y, Deng Y and He Z (2010) Development of novel self-assembled DS-PLGA hybrid nanoparticles for improving oral bioavailability of vincristine sulfate by P-gp inhibition. *J Control Release* **148:**241-248.

Luo Y, Chen D, Ren L, Zhao X and Qin J (2006) Solid lipid nanoparticles for enhancing vinpocetine's oral bioavailability. *J Control Release* **114:**53-59.

Manjunath K and Venkateswarlu V (2005) Pharmacokinetics, tissue distribution and bioavailability of clozapine solid lipid nanoparticles after intravenous and intraduodenal administration. *J Control Release* **107:**215-228.

Mishra VK, Mohammad G and Mishra SK (2008) Downregulation of telomerase activity may enhanced by nanoparticle mediated curcumin delivery. *Digest Journal of Nanomaterials and Biostructures* **3:**163-169.

Mittal G and Kumar MN (2009) Impact of polymeric nanoparticles on oral pharmacokinetics: A dose-dependent case study with estradiol. *J Pharm Sci*.

Mittal G, Sahana DK, Bhardwaj V and Ravi Kumar MN (2007) Estradiol loaded PLGA nanoparticles for oral administration: effect of polymer molecular weight and copolymer composition on release behavior in vitro and in vivo. *J Control Release* **119:**77-85.

Papahadjopoulos D, Allen TM, Gabizon A, Mayhew E, Matthay K, Huang SK, Lee KD, Woodle MC, Lasic DD, Redemann C and et al. (1991) Sterically stabilized liposomes: improvements in pharmacokinetics and antitumor therapeutic efficacy. *Proc Natl Acad Sci U S A* **88:**11460-11464.

Parkinson A., Ogilive B.W., Paris B.L., Hensely T.N. and Loewen G.J. (2010) *Human Biotransformation; In Biotransformation and Metabolite Elucidation of Xenobiotics*. John Wiley & Sons, Inc.

Petros RA and DeSimone JM (2010) Strategies in the design of nanoparticles for therapeutic applications. *Nat Rev Drug Discov* **9:**615-627.

Piskin E, Tuncel A, Denizli A and Ayhan H (1994) Monosize microbeads based on polystyrene and their modified forms for some selected medical and biological applications. *J Biomater Sci Polym Ed* **5:**451-471.

Qian F, Cui F, Ding J, Tang C and Yin C (2006) Chitosan graft copolymer nanoparticles for oral protein drug delivery: preparation and characterization. *Biomacromolecules* **7:**2722-2727.

Roser M, Fischer D and Kissel T (1998) Surface-modified biodegradable albumin nano- and microspheres. II: effect of surface charges on in vitro phagocytosis and biodistribution in rats. *Eur J Pharm Biopharm* **46:**255-263.

Schluep T, Cheng J, Khin KT and Davis ME (2006) Pharmacokinetics and biodistribution of the camptothecin-polymer conjugate IT-101 in rats and tumor-bearing mice. *Cancer Chemother Pharmacol* **57:**654-662.

Scott DO, Bindra DS and Stella VJ (1993) Plasma pharmacokinetics of lactone and carboxylate forms of 20(S)-camptothecin in anesthetized rats. *Pharm Res* **10:**1451-1457.

Sinha R, Kim GJ, Nie S and Shin DM (2006) Nanotechnology in cancer therapeutics: bioconjugated nanoparticles for drug delivery. *Mol Cancer Ther* **5:**1909-1917.

Slepushkin VA, Simoes S, Dazin P, Newman MS, Guo LS, Pedroso de Lima MC and Duzgunes N (1997) Sterically stabilized pH-sensitive liposomes. Intracellular delivery of aqueous contents and prolonged circulation in vivo. *J Biol Chem* **272:**2382-2388.

Takeuchi H, Yamamoto H, Niwa T, Hino T and Kawashima Y (1996) Enteral absorption of insulin in rats from mucoadhesive chitosan-coated liposomes. *Pharm Res* **13:**896-901.

Torche´ AM, Jouan H, Corre PS, Albina E, Primault R, Jestin A, Verge RL and (2000) Ex vivo and in situ PLGA microspheres uptake by pig ileal Peyer's patch segment. *International Journal of Pharmaceutics* **201:**15-27.

Vereczkey L, Czira G, Tamas J, Szentirmay Z, Botar Z and Szporny L (1979) Pharmacokinetics of vinpocetine in humans. *Arzneimittelforschung* **29:**957-960.

Verrecchia T., Spenlehauer G, Bazile DV, Murry-Brelier A, Archimbaud Y and Veillard M (1995) Non-stealth (poly(lactic acid/albumin)) and stealth (poly(lactic acid-

polyethylene glycol)) nanoparticles as injectable drug carriers. *Journal of Controlled Release* **36:**49-61.

Xu F, Yuan Y, Shan X, Liu C, Tao X, Sheng Y and Zhou H (2009) Long-circulation of hemoglobin-loaded polymeric nanoparticles as oxygen carriers with modulated surface charges. *Int J Pharm* **377:**199-206.

Yamamoto Y, Nagasaki Y, Kato Y, Sugiyama Y and Kataoka K (2001) Long-circulating poly(ethylene glycol)–poly(D,L-lactide) block copolymer micelles with modulated surface charge. *Journal of Controlled Release* **77:**27-38.

Zhang C, Newsome JT, Mewani R, Pei J, Gokhale PC and Kasid UN (2009) Systemic delivery and pre-clinical evaluation of nanoparticles containing antisense oligonucleotides and siRNAs. *Methods Mol Biol* **480:**65-83.

Zhang L, Gu FX, Chan JM, Wang AZ, Langer RS and Farokhzad OC (2008) Nanoparticles in medicine: therapeutic applications and developments. *Clin Pharmacol Ther* **83:**761-769.

Zweers ML, Engbers GH, Grijpma DW and Feijen J (2006) Release of anti-restenosis drugs from poly(ethylene oxide)-poly(DL-lactic-co-glycolic acid) nanoparticles. *J Control Release* **114:**317-324.

Footnotes

This work was supported by the National Institutes of Health National Eye Institute [grants RO1-EY017533, RO1-EY018940, RO-1EY017045].

Figure legend

Figure 1. Model predicted and observed concentrations of camptothecin in plasma after intravenous administration in female SD rats. Two compartment model for camptothecin solution and polymer conjugated camptothecin (IT-101). Key: kel, elimination rate constant form the plasma compartment; k12, rate constant for transfer of drug from the plasma compartment to the distribution compartment; k21, rate constant for transfer of drug form the distribution compartment to the plasma compartment.

Figure 2. Model predicted and observed concentrations of 9-nitocamptothecin in plasma after intravenous administration in male Wistar rats. One compartment model for 9-nitocamptothecin solution and two compartment model for polymeric nanoparticles of 9-nitrocamptothecin. Key: kel, elimination rate constant form the plasma compartment; k12, rate constant for transfer of drug from the plasma compartment to the distribution compartment; k21, rate constant for transfer of drug form the distribution compartment to the plasma compartment.

Figure 3. Model predicted and observed concentrations of epirubicin in plasma after intravenous administration in male Wistar rats. Two compartment model for epirubicin solution and three compartment model for self assembled curdalan and cholesterol nanoparticles of epirubicin. Key: kel, elimination rate constant form the plasma compartment; k12, rate constant for transfer of drug from the plasma compartment to the distribution compartment; k21, rate constant for transfer of drug form the distribution compartment to the plasma compartment.; k13, rate constant for transfer of drug from the plasma compartment to the second distribution compartment; k31, rate constant for transfer of drug form the second distribution compartment to the plasma compartment

Figure 4. Model predicted and observed concentrations of vinpocetine in plasma after oral administration in male Wistar rats. One compartment model for vinpocetine solution and two compartment model for vinpocetine solid-lipid nanoparticles. Key: ka, absorption rate constant form GI tract to the plasma, kel, elimination rate constant form the plasma compartment; k12, rate constant for transfer of drug from the plasma compartment to the distribution compartment; k21, rate constant for transfer of drug form the distribution compartment to the plasma compartment.

Figure 5. Model predicted and observed concentrations of clozepine in plasma after intraduodenal and intravenous administration in male Wistar rats. Two compartment model for clozepine suspension and clozepine solid-lipid nanoparticles. Key: ka, absorption rate constant form GI tract to the plasma, kel, elimination rate constant form the plasma compartment; k12, rate constant for transfer of drug from the plasma compartment to the distribution compartment; k21, rate constant for transfer of drug form the distribution compartment to the plasma compartment.

Figure 6. Model predicted and observed concentrations of clozepine nanoparticles in plasma after intraduodenal and intravenous administration in male Wistar rats. Two compartment model for neutral charged solid-lipid nanoparticles and positively charged solid-lipid nanoparticles. Key: ka, absorption rate constant form GI tract to the plasma, kel, elimination rate constant form the plasma compartment; k12, rate constant for transfer of drug from the plasma compartment to the distribution compartment; k21, rate constant for transfer of drug form the distribution compartment to the plasma compartment

Figure 7. Model predicted and observed concentrations of cyclosporine-A in plasma after oral administration in male Beagle dogs. Two compartment model for negatively charged and positively charged nanoparticles. Key: ka, absorption rate constant form GI tract to the plasma, kel, elimination rate constant form the plasma compartment; k12, rate constant for transfer of drug from the plasma compartment to the distribution compartment; k21, rate constant for transfer of drug form the distribution compartment to the plasma compartment

Table 1. Drug name, nanoparticle composition, particle size, surface charge, route of administration, species of study, and dose of nanoparticles used for pharmacokinetic parameter estimations in this study. Key: NA – not available; NP – nanoparticle.

Drug Name	**Matrix Material of Nanoparticles**	**Particle Size (nm)**	**Particle Charge**	**Route**	**Species**	**Dose Administered**	**Reference**
Camptothecin IT-101	Polymer conjugate of camptothecin and beta-cyclodextrin based polymer	78	NA	Intravenous	Female Sprague Dawley Rats	1 mg/ kg	(Schluep et al., 2006)
9-Nitrocamptothecin	Nanoparticles made with PLGA (50:50) and polyvinyl alcohol (PVA)	207 ± 26	NA	Intravenous	Male Wistar Rats	2 mg/kg	(Dadashzadeh et al., 2008)
Epirubicin	Self-assembled system made with carboxymethyl curdlan coupled with cholesterol chitosan	208	Negative (-32.1)	Intravenous	Male Wistar Rats	10 mg/kg	(Li et al., 2010)
Vinpocetine	Solid lipid nanoparticles made with glycerol monostearate, polysorbate 80 and soya lecithin	70.3 ± 7.8	Negative (-33.8 ± 0.9)	Oral	Male Wistar Rats	10 mg/kg	(Luo et al., 2006)

Clozepine	Solid lipid nanoparticles made with triglyceride, phosphatidylcholine and poloxomer 188	163 ± 0.7	Positive (+23.2 ± 0.9)	Duodenal and Intravenous	Male Wistar Rats	20 mg/kg	(Manjunath and Venkateswarlu, 2005)
Cyclosporine A (Positively Charged NP)	Nanoparticles made with lecithin, poloxamer 188 and chitosan	148 ± 29	Positive (+31.2 ± 1.6)	Oral	Male Beagle Dogs	7.5 mg/kg	(El-Shabouri, 2002)
Cyclosporine A (Negatively Charged NP)	Nanoparticles made with lecithin, poloxamer 188 and sodium glycocholate	104 ± 18	Negative (-41.6 ± 1.1)	Oral	Male Beagle Dogs	7.5 mg/kg	(El-Shabouri, 2002)

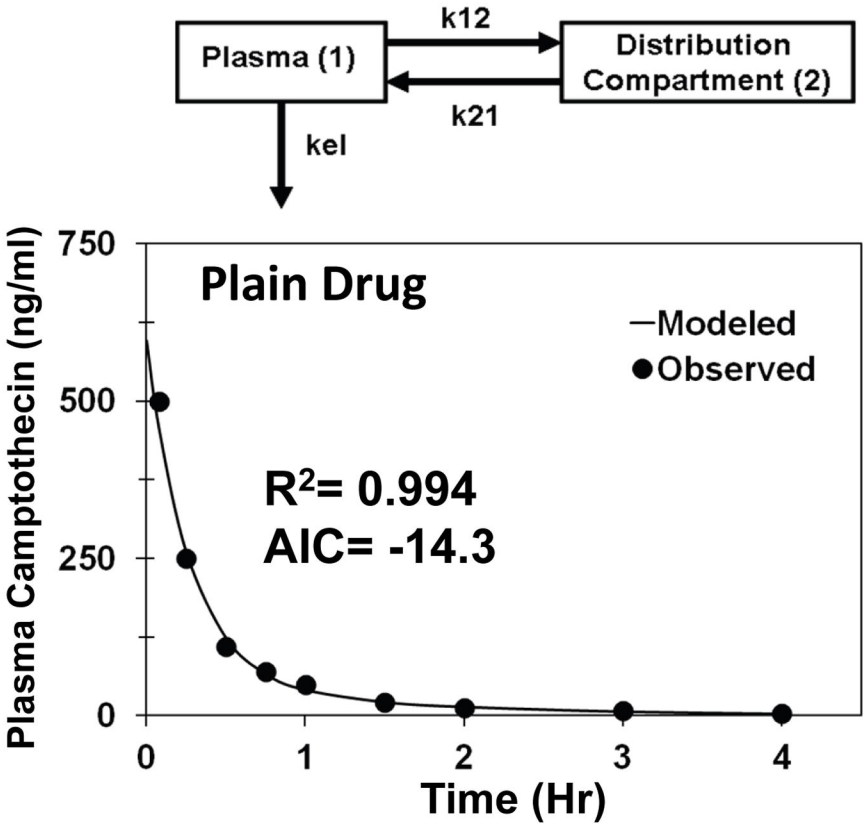

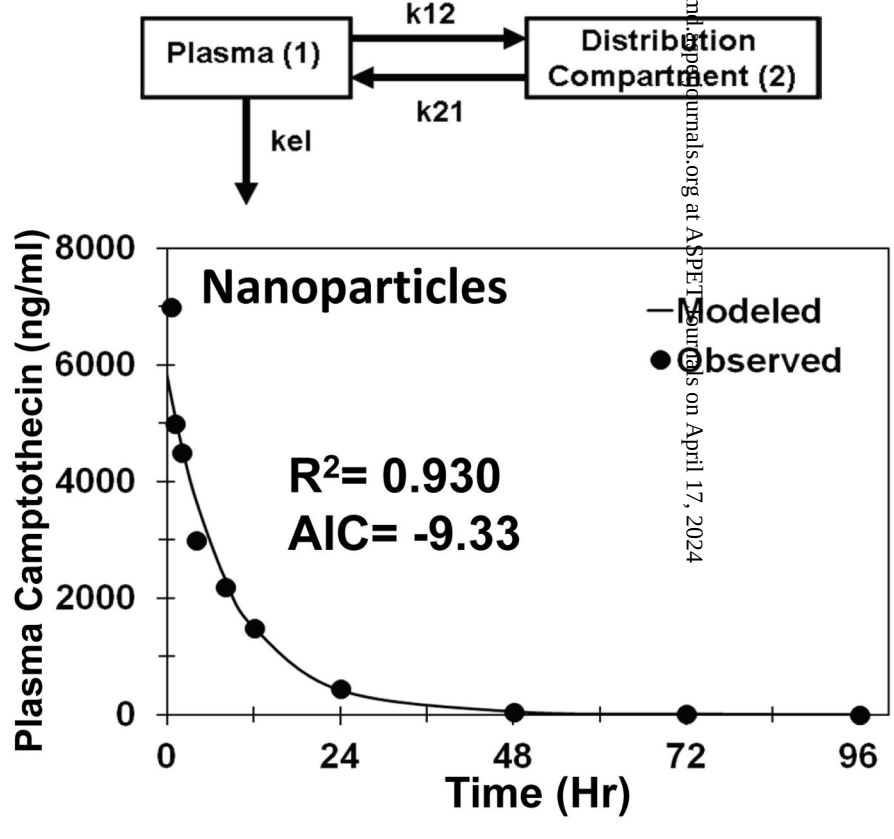

	kel (h^{-1})	V (L)	CL (L/h)	k12 (h^{-1})	k21 (h^{-1})	ß (h^{-1})	$t_{½}$ (h)
Nanoparticles	0.109	0.151	0.0165	0.006	0.040	0.037	18.73
Plain Drug	2.62	1.68	4.39	0.81	0.98	0.69	1.0

Figure 1

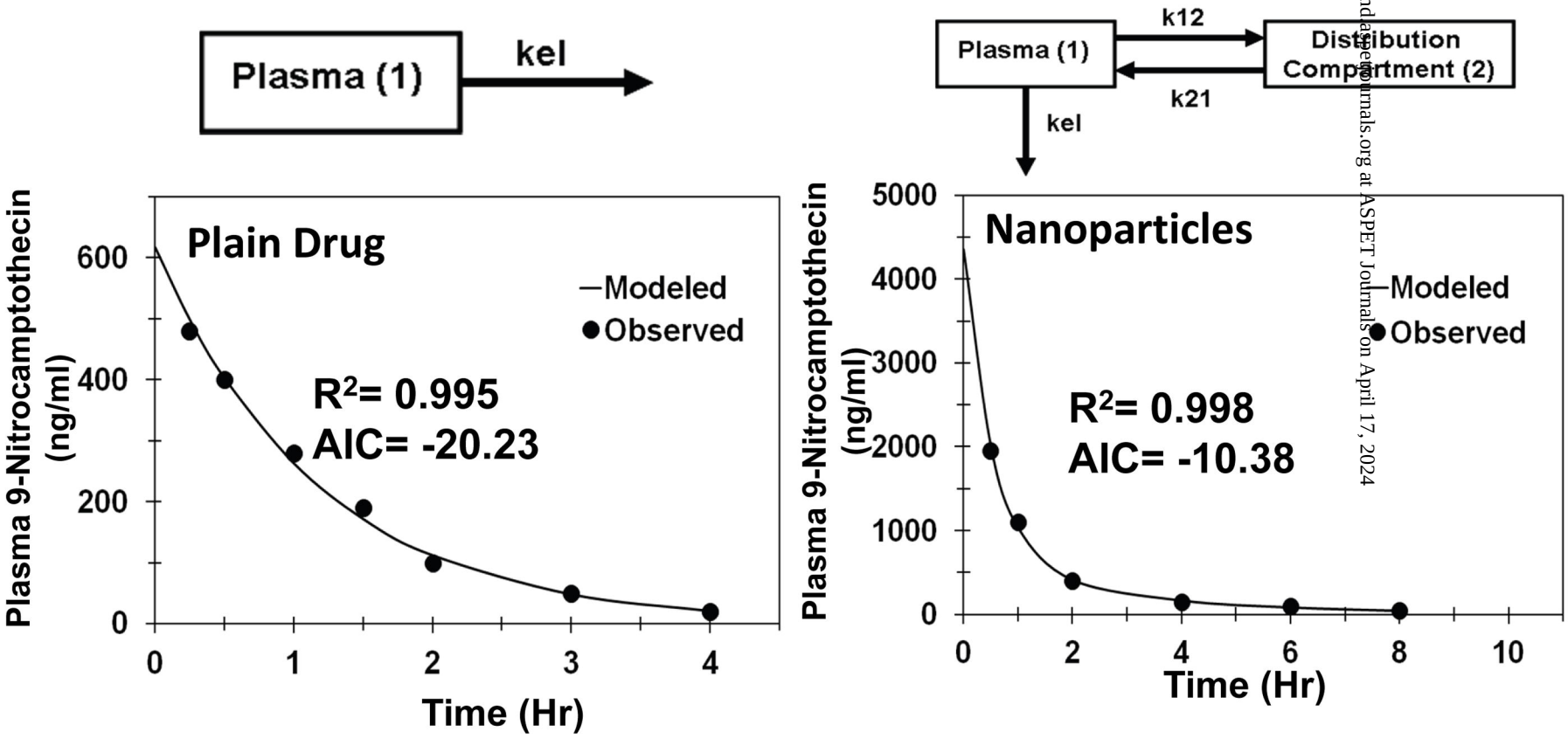

	kel (h^{-1})	V (L)	CL (L/h)	k12 (h^{-1})	k21 (h^{-1})	ß (h^{-1})	$t_{1/2}$ (h)
Nanoparticles	1.12	0.459	0.480	0.510	0.549	0.334	2.08
Plain Drug	0.854	3.24	2.96	NA	NA	NA	0.811

Figure 2

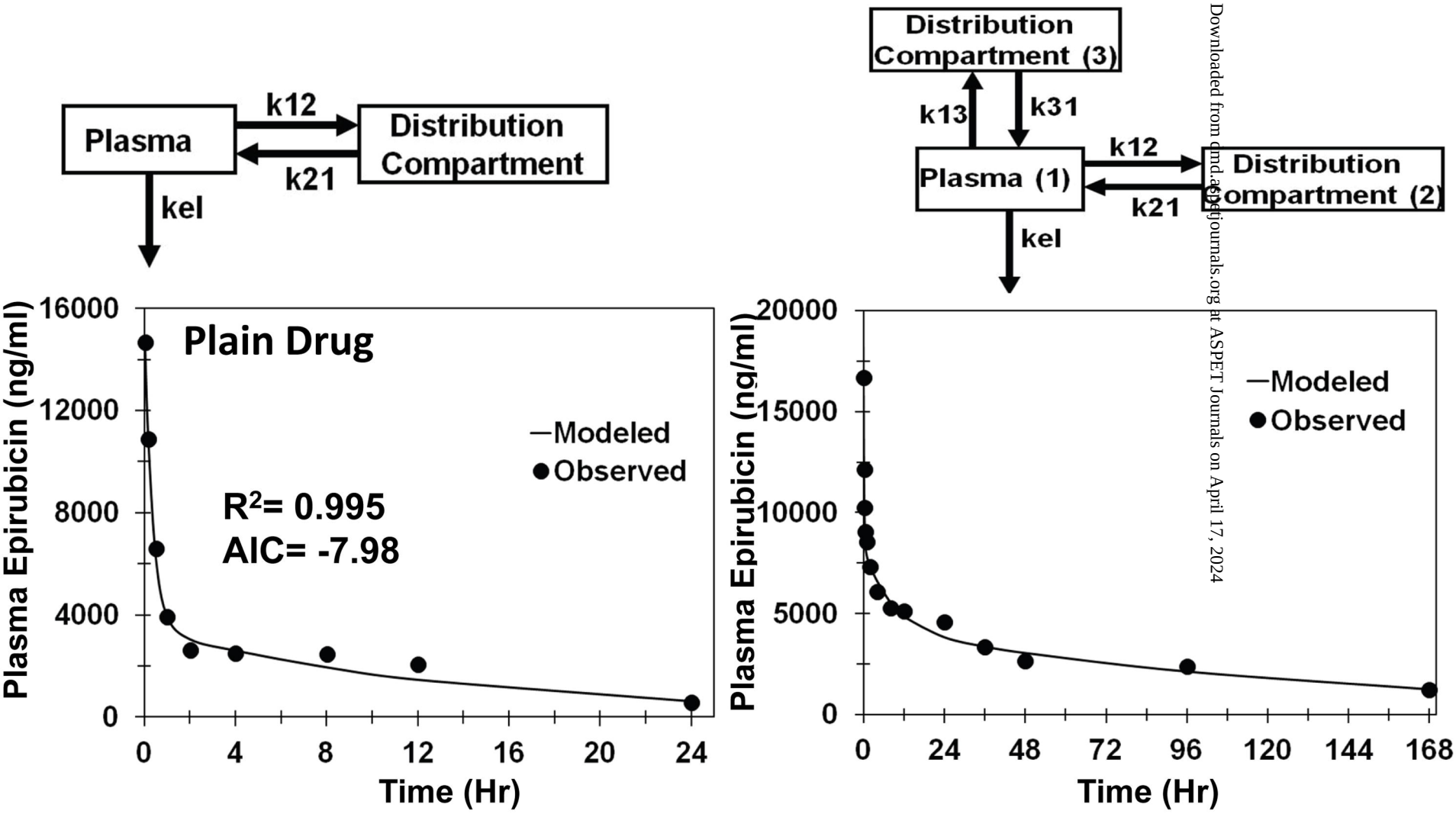

	kel (h^{-1})	V (L)	CL (L/h)	k12 (h^{-1})	k21 (h^{-1})	k13 (h^{-1})	k31 (h^{-1})	ß (h^{-1})	$t_{½}$ (h)
Nanoparticles	0.029	0.549	0.016	0.110	0.068	2.96	2.62	0.010	69.3
Plain Drug	0.301	0.635	0.191	1.93	0.683	NA	NA	0.072	9.57

Figure 3

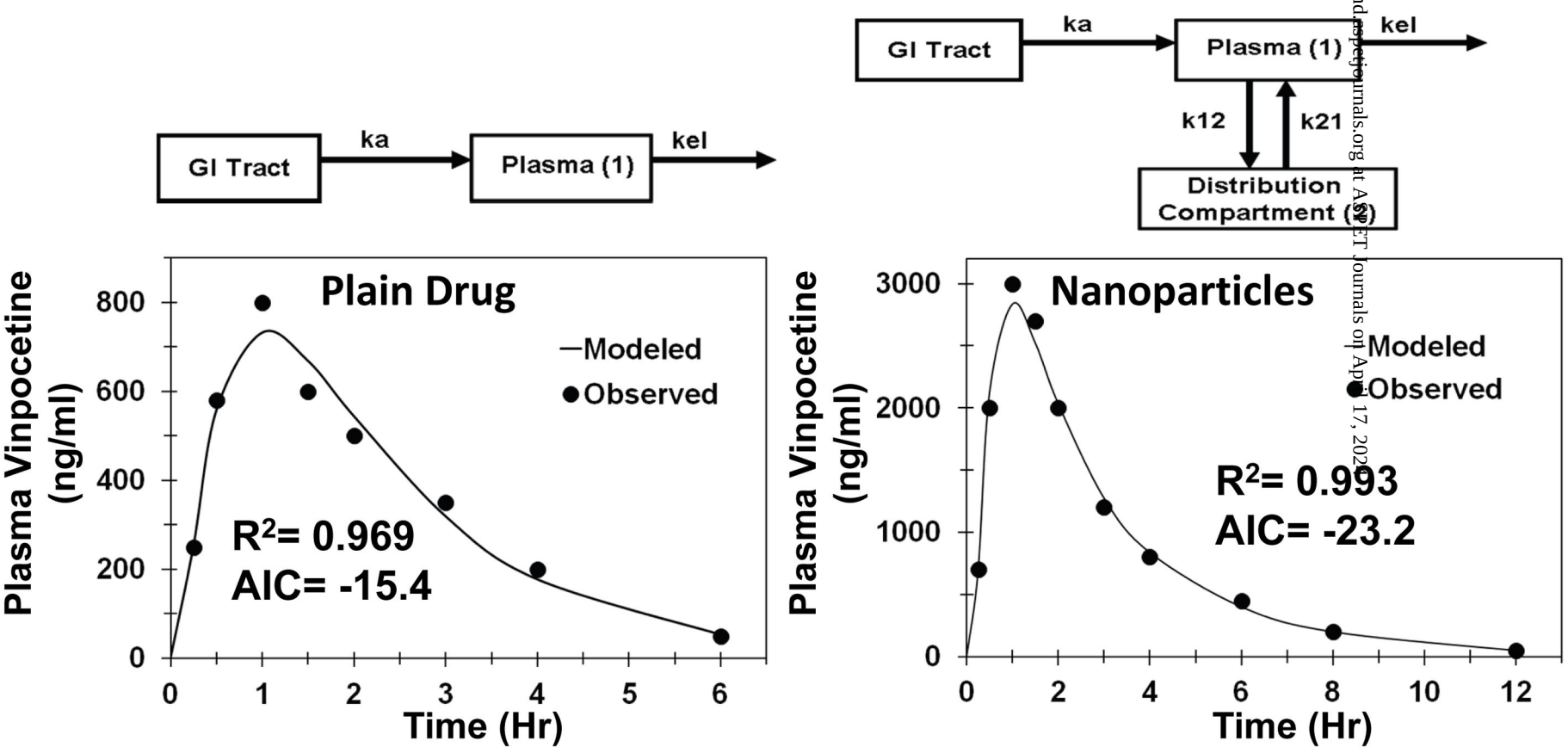

	ka (h^{-1})	kel (h^{-1})	V/F (L)	CL/F (L/h)	k12 (h^{-1})	k21 (h^{-1})	ß (h^{-1})	$t_{½}$ (h)
Nanoparticles	1.61	0.682	1.59	1.08	0.464	0.811	0.343	2.02
Plain Drug	0.610	1.83	2.63	4.81	NA	NA	NA	1.14

Figure 4

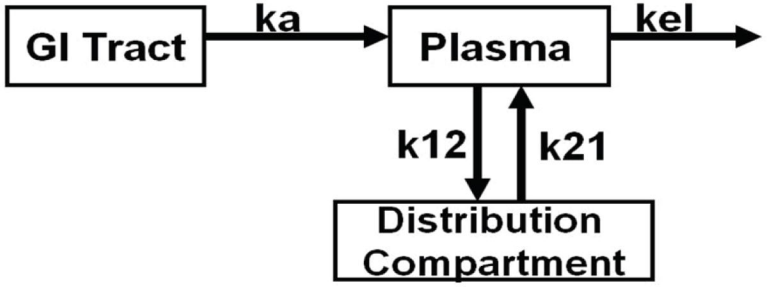

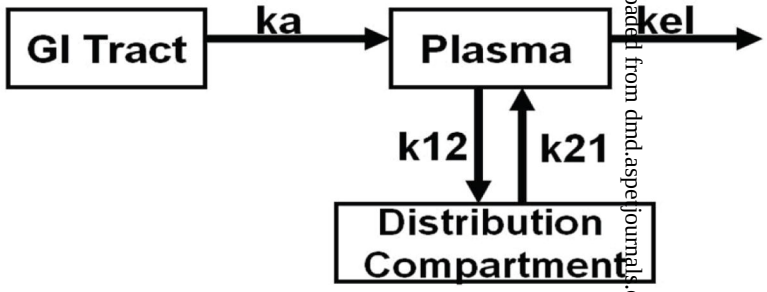

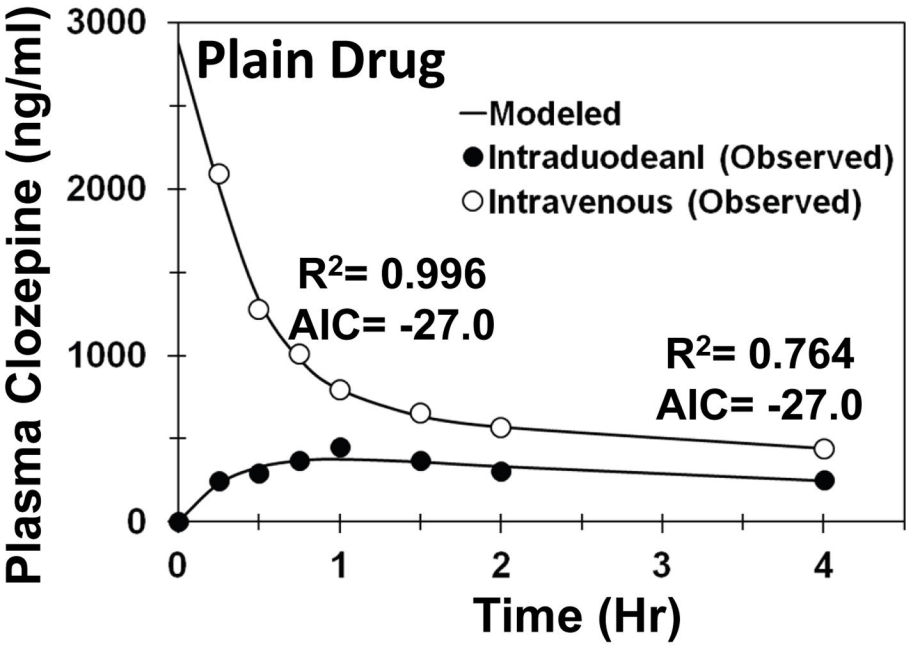

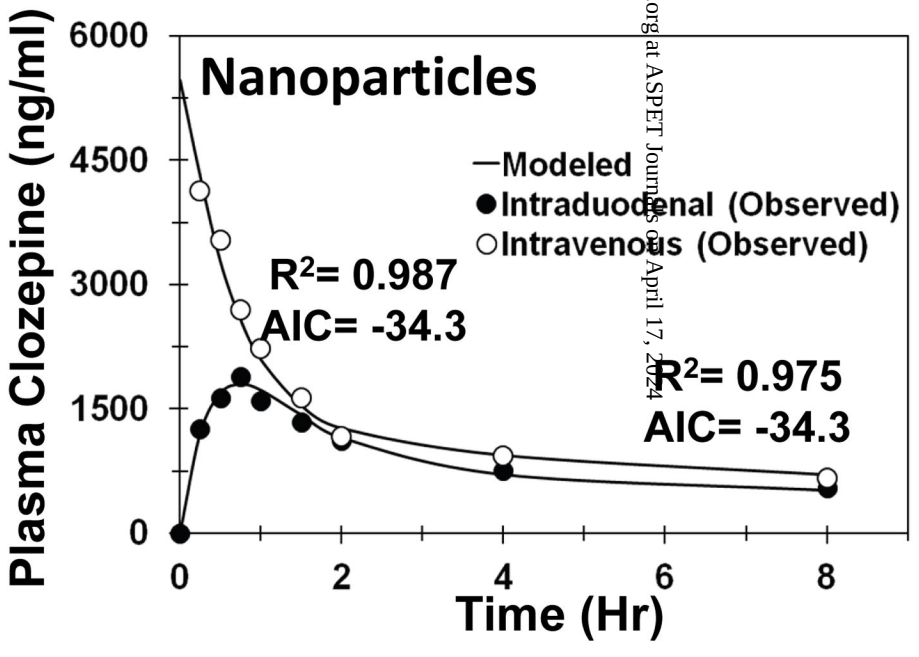

	ka (h^{-1})	kel (h^{-1})	V (L)	CL (L/h)	k12 (h^{-1})	k21 (h^{-1})	ß (h^{-1})	$t_{½}$ (h)	F
Nanoparticles (IV)	NA	0.280	1.72	0.48	0.97	0.39	0.069	9.99	NA
Plain Drug(IV)	NA	0.486	3.0	1.42	1.68	0.66	0.116	5.95	NA
Nanoparticles (ID)	1.74	0.280	1.72	0.48	0.97	0.39	0.069	9.99	0.35
Plain Drug (ID)	0.831	0.486	3.0	1.42	1.68	0.66	0.116	5.95	0.23

Figure 5

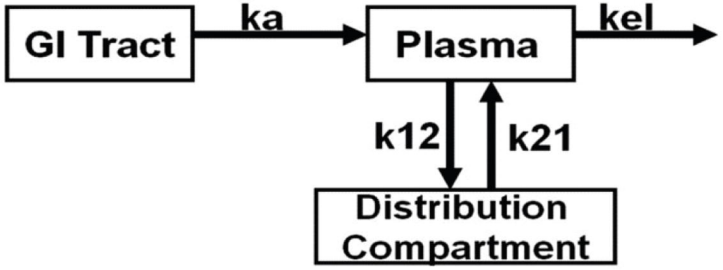

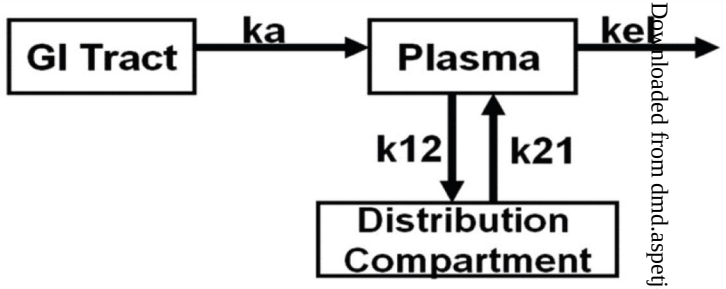

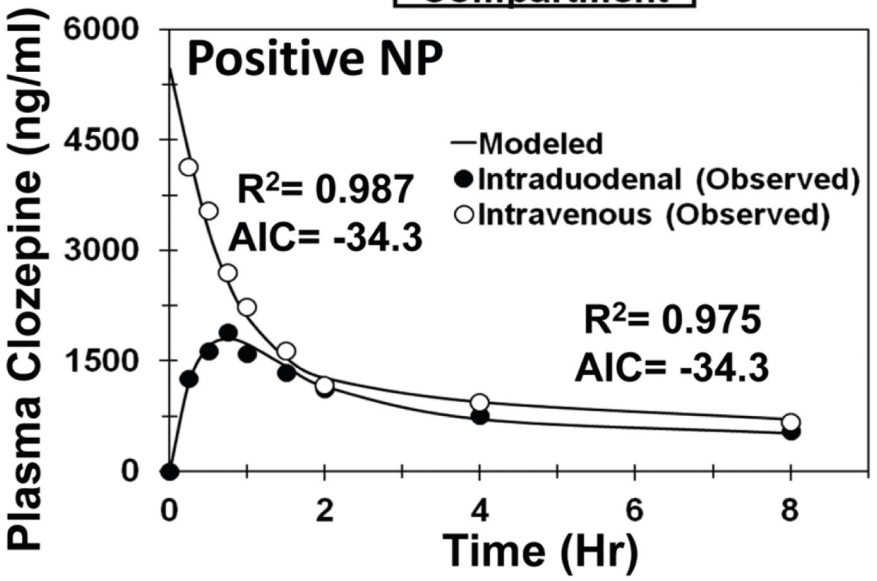

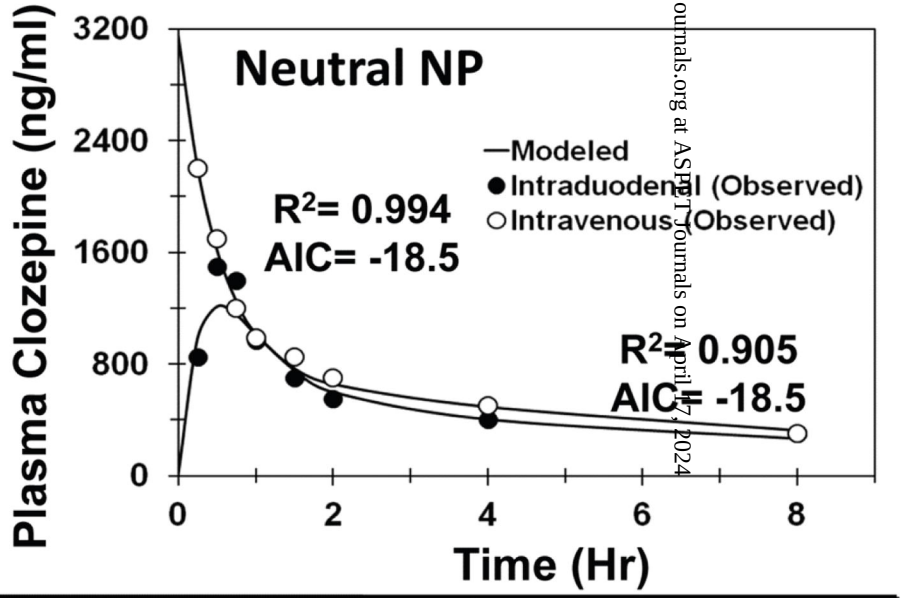

	ka (h^{-1})	kel (h^{-1})	V (L)	CL (L/h)	k12 (h^{-1})	k21 (h^{-1})	ß (h^{-1})	$t_{½}$ (h)	F
Nanoparticles- IV (Positive)	NA	0.280	1.72	0.48	0.97	0.39	0.069	9.99	NA
Nanoparticles- IV (Neutral)	NA	0.372	3.17	1.18	1.13	0.54	0.103	6.73	NA
Nanoparticles- IV (Positive)	1.74	0.280	1.72	0.48	0.97	0.39	0.069	9.99	0.35
Nanoparticles- IV (Neutral)	2.66	0.372	3.17	1.18	1.13	0.54	0.103	6.73	0.39

Figure 6

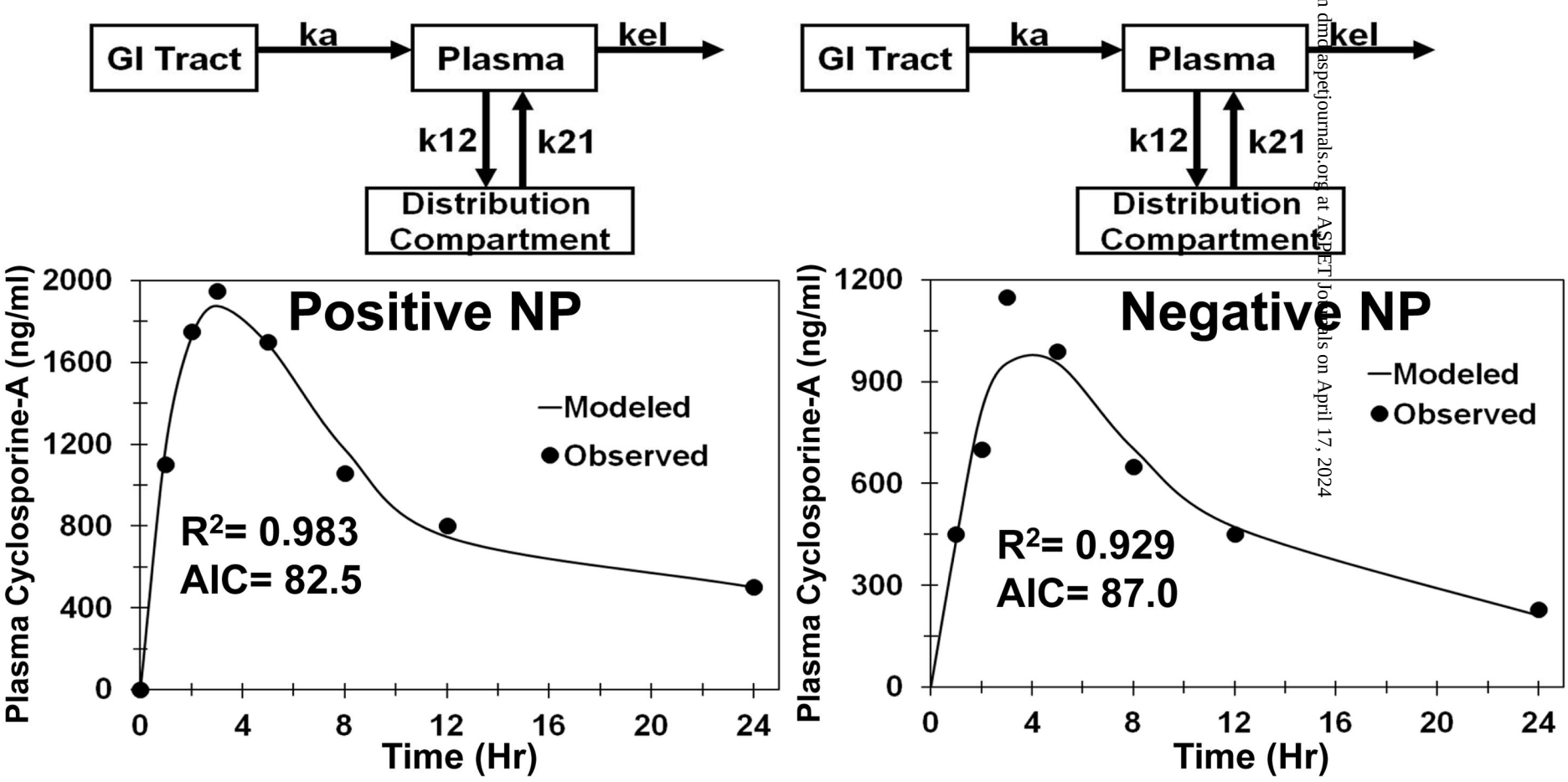

	ka (h^{-1})	kel (h^{-1})	V/F (L)	CL/F (L/h)	k12 (h^{-1})	k21 (h^{-1})	ß (h^{-1})	$t_{½}$ (h)
Positive NP	0.334	0.104	1.50	0.156	0.337	0.036	0.008	85.5
Negative NP	0.229	0.250	1.82	0.455	0.260	0.054	0.025	27.7

Figure 7